LETTERS

Remobilization of southern African desert dune systems by twenty-first century global warming

David S. G. Thomas[1], Melanie Knight[2] & Giles F. S. Wiggs[1]

Although desert dunes cover 5 per cent of the global land surface and 30 per cent of Africa, the potential impacts of twenty-first century global warming on desert dune systems are not well understood[1]. The inactive Sahel and southern African dune systems, which developed in multiple arid phases since the last interglacial period[2], are used today by pastoral and agricultural systems[3,4] that could be disrupted if climate change alters twenty-first century dune dynamics. Empirical data and model simulations have established that the interplay between dune surface erodibility (determined by vegetation cover and moisture availability) and atmospheric erosivity (determined by wind energy) is critical for dunefield dynamics[5]. This relationship between erodibility and erosivity is susceptible to climate-change impacts. Here we use simulations with three global climate models and a range of emission scenarios to assess the potential future activity of three Kalahari dunefields. We determine monthly values of dune activity by modifying and improving an established dune mobility index[6] so that it can account for global climate model data outputs. We find that, regardless of the emission scenario used, significantly enhanced dune activity is simulated in the southern dunefield by 2039, and in the eastern and northern dunefields by 2069. By 2099 all dunefields are highly dynamic, from northern South Africa to Angola and Zambia. Our results suggest that dunefields are likely to be reactivated (the sand will become significantly exposed and move) as a consequence of twenty-first century climate warming.

Dune sand transport is significantly inhibited or prevented by vegetation cover of over 14% (ref. 7). Cover varies with position on the dune—flanks are normally better vegetated than crests owing to soil moisture distributions and degree of exposure to wind events. There is also significant short-term variation in subtropical dune system dynamics because of high interannual rainfall variability, droughts, localized fire and human impacts[8]. These can reduce vegetation cover on crests and flanks to less than 14%, leading to aeolian (wind-borne) sediment mobilization[5], until vegetation recovers and crestal stabilization ensues[9]. This century, global warming is widely predicted to lead to reductions in net soil moisture and an increase in high-magnitude climatic events, including droughts in the subtropics[10]. Persistent changes in mean climatic parameters affecting soil moisture and windiness (which affect erodibility and erosivity) are most likely to markedly affect dunefield activity. Erodibility relates to vegetation and biocrusts and therefore to effective moisture ($P - E_p$, where P is precipitation and E_p is potential evapotranspiration), and erosivity relates to the aeolian transport capacity, expressed as the cube of mean wind speed, $\bar{U}^3$ (refs 11, 12).

In the southern Kalahari today, low wind energy limits potential sand transport to higher linear dune slopes and crests, where vegetation cover controls whether dune sand transport and erosion takes place[13]. Eastern and northern dunefields are well vegetated and largely buffered from erosivity effects[5]. To assess twenty-first century dunefield dynamics we developed a methodology for using General Climate Model (GCM) data and an indexed measure of surface erodibility and erosivity. With a methodology established and tested, we applied it to data from a range of GCM scenarios for the three central southern African Kalahari dunefields (Fig. 1).

Monthly GCM outputs were used to assess future changes in intra-annual dune activity. Several indices of dune mobility exist that include erodibility and erosivity parameters defined by climate data[14–16]. $M = W/(P/E_p)$, where W is the percentage of the time wind is above the threshold for sand transport, was first applied in the Kalahari[6], with subsequent applications and calibration in other

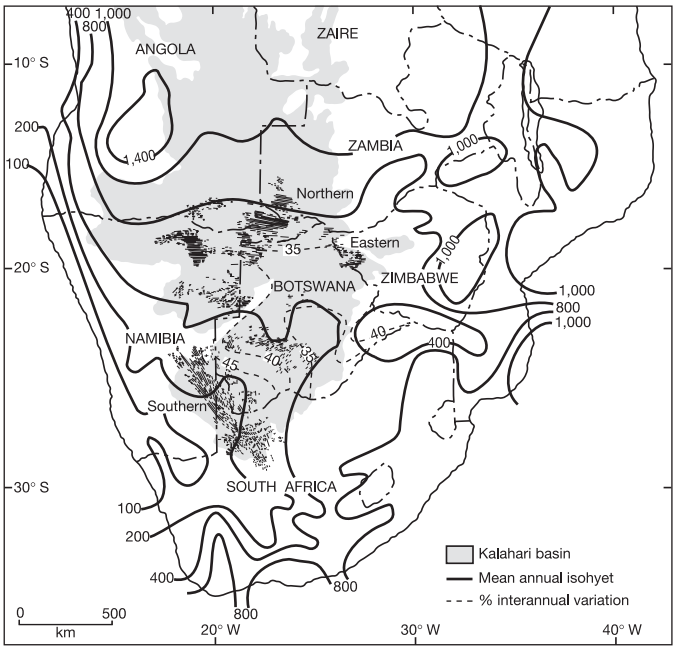

Figure 1 | The southern African Kalahari basin and dune systems. Mean annual rainfall and interannual rainfall variability isolines are shown. Most rainfall occurs October–April. In the driest, southern, areas dunes have a partial vegetation cover that responds to the high interannual rainfall variability. Low wind energy today limits sand transport and vegetation recovers after dry periods to impart stability, except where land-use pressures create bare hotspots of activity. In northern and eastern areas dunes are heavily vegetated, including supporting mixed deciduous woodland in places, owing to higher precipitation levels. Modelled 1961–90 mean $A_{p,GCM}$ values correctly predict dune inactivity throughout the Kalahari. Isohyet, lines of equal precipitation.

[1]School of Geography and Environment, Oxford University Centre for the Environment, University of Oxford, South Parks Road, Oxford OX1 3QY, UK. [2]Department of Earth and Life Sciences, University of Salford, Manchester M5 4WT, UK.

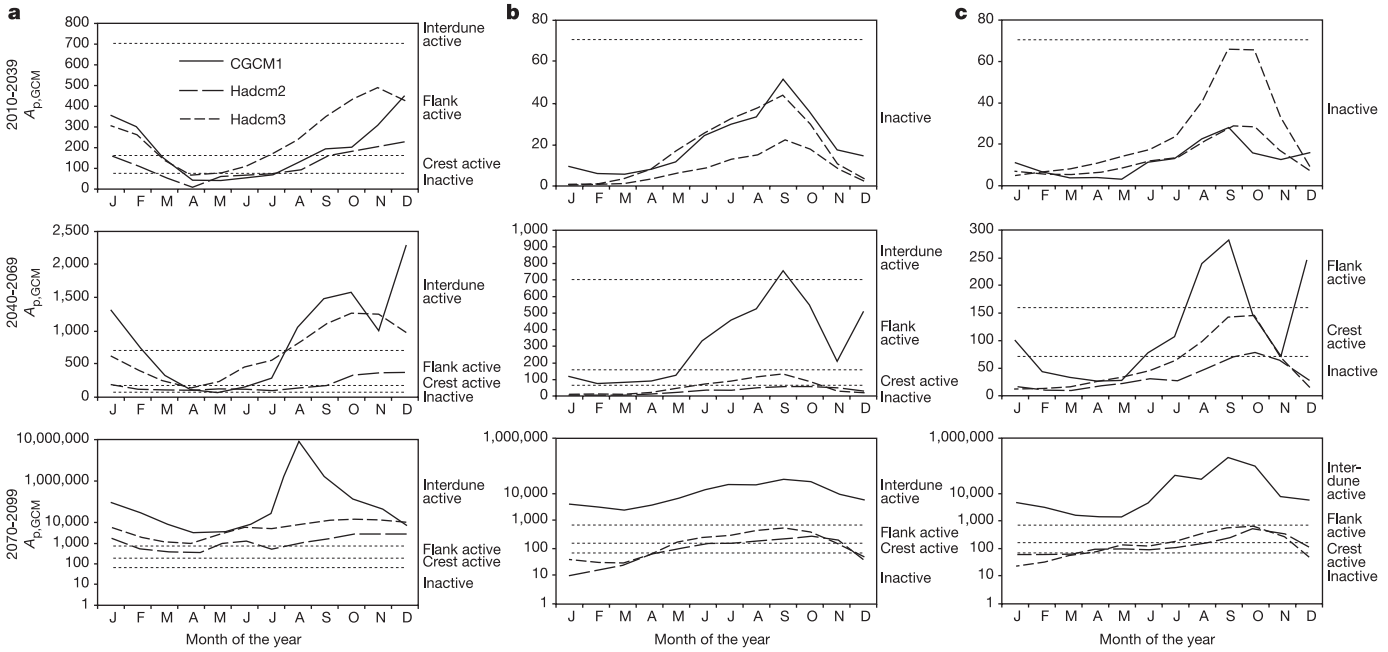

Figure 2 | $A_{p,GCM}$ dune mobility predictions using IS92a ($2 \times CO_2$) emissions scenarios. Data are shown as average annual monthly activity within each tridecadal period. **a**, Southern dunefield; **b**, northern dunefield; **c**, eastern dunefield. By 2070, dune flank activity is predicted by all model outcomes in the southern dunefield (bottom panel of **a**). Significantly, interdune activity, indicating a fully active dunefield, is predicted in two scenarios. In the northern Kalahari, significant activity is also predicted after 2040 (middle panel of **b**), suggesting a marked change in landscape stability and ecosystems.

dunefields[17,18]. We modified the index M to account for GCM data outputs and to determine monthly values, improving sensitivity in a region of highly seasonal climate (see Methods). GCMs were evaluated to provide twenty-first century climate predictions, with consideration given to grid sizes, ability to postdict the 1961–90 climate for index validation, and sensitivity to atmospheric composition and level of greenhouse gases[19]. Hadcm3, Hadcm2 and CGCM1 were selected for their relatively fine resolutions, with predictions of future global warming ranging from 2.5 °C (Hadcm3) to 3.5 °C (CGCM1) by 2100. These GCMs allowed different model generations to be incorporated into the study. Testing indicated that no one GCM performed well for all key variables, but for Hadcm3 and Hadcm2, values of the revised index of potential dune activity, $A_{p,GCM}$ (see Methods for definition) bore a close relationship to those derived from observed data for the 1961–90 period. Monthly and annual GCM data runs were used for future climate scenarios, with results averaged over tridecadal blocks (2010–2039, 2040–2069 and 2070–2099). We used the IS92a ($2 \times CO_2$) emission scenario and several SRES scenarios to account for increases in additional atmospheric gases[20]. Once predictions were made for the erosivity and erodibility elements of $A_{p,GCM}$, the results were analysed to consider the impacts of spatial and seasonal[21] trends in future climate.

Using IS92a, all the GCMs produced twenty-first century climate scenarios leading to increased dunefield erodibility, though with differing changes in P and E_p. Csiro-mk2b predicts a doubling of E_p throughout southern Africa by 2100. The older CGCM1 predicts a 50% decline in summer rainfall in northern areas, accompanied by a quadrupling of E_p. Although the newer Hadley GCMs predict smaller increases in E_p than the other models, the P/E_p ratio was always <1. This negative moisture budget applies even to the currently heavily vegetated northern dunefield, for which using SRES emission scenarios Hadcm3 predicts a 50% precipitation increase. When compared, the IS92a and SRES results agree, in that any modelled annual precipitation increases in the southern African interior are outweighed by evapotranspiration increases. Some changes in rainfall seasonality are modelled, but only Csiro-mk2b with SRES scenarios suggests a heightening of dry–wet season contrasts.

Erosivity is projected to increase in all model and scenario outputs, with greatest increases in the southern dunefield. The most sensitive outputs are generated by Hadcm3 with both IS92a and SRES. Ramped erodibility increases are driven by a doubling of the present

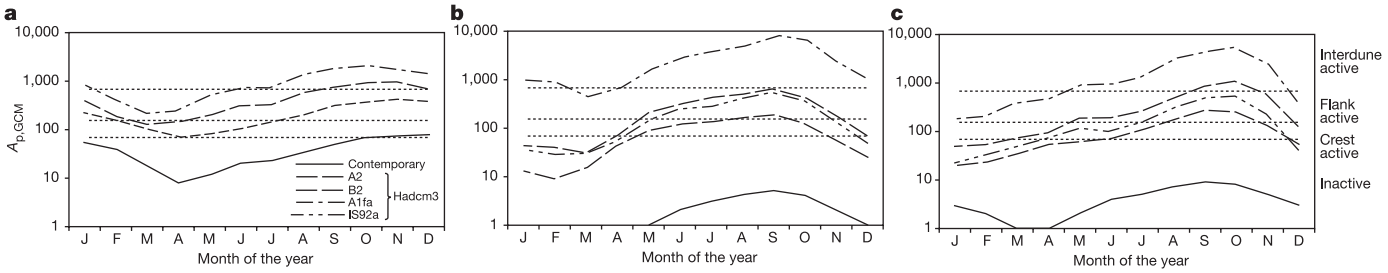

Figure 3 | Contemporary and post 2070 $A_{p,GCM}$ values of Kalahari dunefield activity. **a**, Southern dunefield; **b**, northern dunefield; **c**, eastern dunefield. 'Contemporary' indicates values calculated using 1961–90 climate data. Post-2070 runs with the Hadcm3 GCM use a range of emission scenarios: A2, SRES 'business as usual' emissions; B2, SRES medium emissions scenario; A1fa, SRES emissions with increasing fossil fuel use; IS92a, the $2 \times CO_2$ scenario.

mean wind speeds to 4 m s^{-1} after 2040. Little change occurs in the timing of wind-speed maxima throughout the year, with the focus remaining in the August–October period.

To establish potential future dunefield activity we integrated temporal determinations of erodibility and erosivity from specific GCM and emission scenarios into $A_{p,GCM}$. Under the present climate conditions, only the southern dunefield experiences activity and this is largely limited to dune crests during droughts[7]. All modelled outputs project marked increases in dune activity during the twenty-first century in all dunefields, including after 2040 in the northern dunefield (Botswana, Namibia, Angola) and in the eastern dunefield (Zimbabwe, Zambia). Significantly, by 2070 activity levels even in northern areas exceed the current activity maxima in the dry southwestern areas. No particular GCMs or emission scenarios consistently produce the 'least active' or 'most active' predictions, but with IS92a emissions CGCM1 often produces the most active scenarios (Fig. 2).

The GCMs all produce increasing levels of activity over the twenty-first century, including fully active dunefields, where interdune areas are devegetated and sand mobility and transfer between dunes is possible, resulting in marked landscape changes such as plant community diminutions. These would represent considerable, even catastrophic, limitations on the present agricultural uses of these environments. Our model does not account for the potential impact of enhanced atmospheric CO_2 levels on plant productivity, which may be greatest in dry environments[22]. These might counter some of the cover reductions due to reduced future net precipitation; however, critical advantages may be lost under the impacts of droughts that are expected to increase in severity and frequency[23]. From the middle of the twenty-first century projected values of $A_{p,GCM}$ are exceedingly high (>5,000 in many months with several GCM runs) owing to both substantial moisture depletion and markedly enhanced windiness.

We evaluated differing emission scenario impacts on potential dune activity (Fig. 3). Although the extreme situation generated by the use of the SRES A1fa scenario is notable, perhaps of greater significance is that even the medium-emission scenario, B2, generates significant aeolian dynamism across the Kalahari, including the currently heavily vegetated eastern and northern dunefields. The limited southern dunefield activity today displays year-to-year fluctuations in association with climate variability[9]; interannual variability in dune activity levels is modelled to continue in the late twenty-first century too, but even in the least active years $A_{p,GCM}$ values are sufficiently high that dune crests would remain active. If these predictions were to be correct, there would be little respite from sand mobility in the Kalahari dunefields even during relatively moist years.

Finally, we took $A_{p,GCM}$ outputs for the post-2070 period using Hadcm3 and determined the mean status of runs using all four of the emission scenarios used in this analysis (Fig. 4). This indicates that the Kalahari has the potential to achieve levels of aeolian activity that have not operated since 14–16 kyr ago—the last period of

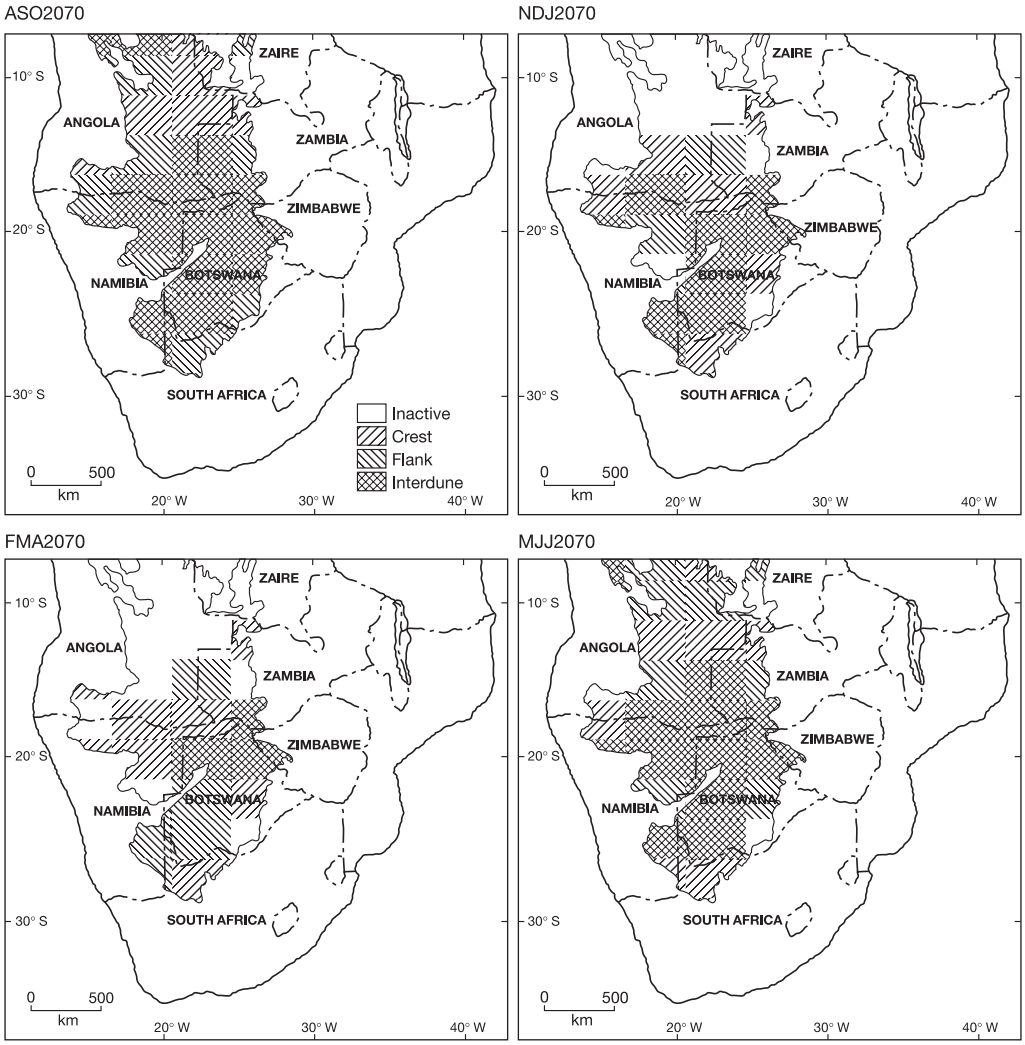

Figure 4 | Predicted three-month block dunefield activity after 2070. This is modelled as the mean of Hadcm3 runs using IS92a, A2, A1fa and B2 emission scenarios. Significant dunefield activity occurs all year round in all three dunefields.

Kalahari-wide dunefield activity recorded in the luminescence-dated sedimentary record[24].

Our findings show that dunefields are likely to experience significant reactivations as a consequence of twenty-first century climate change. This finding is independent of the GCM or emission scenario used. There are uncertainties within the modelled Kalahari scenarios but the general trend and the magnitude of possible changes in the erodibility and erosivity of dune systems suggests that the environmental and social consequences of these changes will be drastic.

METHODS

Potential activity index. To adapt M^6 to GCM data and apply it to a highly seasonal climate regime, several changes were made. Because mean monthly wind velocity, U (in m s^{-1}), is the common GCM wind output, W was replaced by $\bar{U}^3$, which has been employed in other dune mobility indices[14,15], and is widely used in agricultural wind erosion models[11,25], and in investigations of short-event-based sand flux[12]. At present vegetated dunes extend 10° latitude north of the arid southern Kalahari, where M was developed; these northerly locations today receive up to 900 mm of precipitation per year. The moisture retention capacity of dune bodies[26] allows for the more persistent impact of prolonged wet (and dry) periods on soil moisture and vegetation cover through the year[27]. A first-approximation weighting for rainy season net precipitation was therefore introduced, as well as one for the preceding two months rainfall[16]. This weighting is also likely to have a conservative effect on predicted mobility, through its effect on erodibility. The revised index is $A_{p,GCM} = \bar{U}^3/(P_{lag}/E_{p,lag} + P_{rainy}/E_{p,rainy})$, where $\bar{U}^3$ = the cube of the mean wind speed. $P_{lag}/E_{p,lag}$ is the residual effect of recent rainfall and potential evaporation, such that $P_{lag} = (P_{-1} + P_0)/2$, where P_{-1} is precipitation in the previous month and P_0 is rainfall in the current month, and $E_{p,lag} = (E_{p,-1} + E_{p,0})/2$, where $E_{p,-1}$ is potential evapotranspiration in the previous month and $E_{p,0}$ is potential evapotranspiration in the current month. $P_{rainy}/E_{p,rainy}$ is the effect of rainy season precipitation and potential evaporation on soil moisture, such that $P_{rainy} = (P_N + P_D + P_{J...})/m$ and $E_{p,rainy} = (E_{p,N} + E_{p,D} + E_{p,J...})/m$, where m = N (November), D (December), J (January), and so on (abbreviations as in the figures) is the month under consideration within the rainy season. $A_{p,GCM}$ is adapted for the limitations of GCM data outputs, is specifically developed for the seasonal nature of southern African climates, and contains determinations of erodibility and erosivity elements that are not expected to overestimate potential dune dynamics.

Model validation. For dune activity indices the thresholds between classes are important for model calibration. A fourfold division of $A_{p,GCM}$ values was achieved through a validation exercise that explains different levels of aeolian activity within dunefields: $A_{p,GCM} > 700$ indicates highly dynamic dune landscapes, bare dune bodies and sparsely vegetated interdunes; $A_{p,GCM} = 160$–700 indicates significant dune activity, dunes crests bare, dune flanks rippled but moderate interdune vegetation cover; $A_{p,GCM} = 70$–160 indicates dune activity limited to crests, dune flanks vegetated, interdunes well vegetated; and $A_{p,GCM} < 70$ indicates vegetation cover across the whole dune, dunes inactive. Contemporary tridecadal (1961–90) $A_{p,GCM}$ values for the southern dunefield correctly indicate mean dunefield inactivity (Fig. 3); for the northern dunefield $A_{p,GCM} < 10$ for all months, <50 for the eastern dunefield and up to 100 for the southern dunefield. Within these data, high interannual climatic variability (Fig. 1) and rainfall seasonality leads to variations in Kalahari activity status[9,16].

Validation was achieved using monthly $A_{p,GCM}$ values from 1960–2000 climatic data from Twee Riverien in the southern dunefield, calibrated against temporally referenced empirical dune activity and vegetation cover data from published and field research sources. $A_{p,GCM}$ values from >9,000 to 1 were calibrated against: (1) empirical vegetation cover data for September 1999 and June 2000; (2) dune surface activity data based on eight years (1992–2000) repeat dry-season measurements and observations at a number of sites within 10 km of the meteorological station, including published data for 1992 (ref. 7); (3) a photographic library of dune images from 1983–2000 providing further evidence of vegetation conditions on a range of linear dune and interdune areas; and (4) remote sensing and field-based analyses of vegetation cover in the dunefields[28,29], including detailed analyses of two Thematic Mapper satellite image subscenes centred on Twee Riverien in the southern dunefield (1984 and 1993)[9]. Supplementary Fig. 1 illustrates and exemplifies the calibration. In addition, monthly $A_{p,GCM}$ values from 2001–2 automatic weather station data in the very arid, active, negligibly vegetated Namib dunefield, always exceed 31×10^6. Projected values for the southern Kalahari dunefield attain 88×10^6 for August in 2070–2099 with one GCM scenario (Fig. 2).

Received 7 October 2004; accepted 3 May 2005.

1. Thomas, D. S. G. in *Arid Zone Geomorphology* (ed. Thomas, D. S. G.) 373–412 (Wiley, Chichester, 1998).
2. Stokes, S., Thomas, D. S. G. & Washington, R. Multiple episodes of aridity in southern Africa since the last interglacial period. *Nature* **388,** 154–158 (1997).
3. Sporton, D. & Thomas, D. S. G. *Sustainable Livelihoods in Kalahari Environments. Contributions to Global Debates* (OUP, Oxford, 2002).
4. Turner, M. D. Spatial and temporal scaling of grazing impact on the species composition and productivity of Sahelian annual grasslands. *J. Arid Environs* **41,** 277–297 (1999).
5. Livingstone, I. & Thomas, D. S. G. in *The Dynamics and Context of Aeolian Systems* (ed. Pye, K.) 91–101 (Geol. Soc. Spec. Pub. 72, Geological Society, London, 1993).
6. Lancaster, N. Development of linear dunes in the southwestern Kalahari, southern Africa. *J. Arid Environs* **14,** 233–244 (1988).
7. Wiggs, G. F. S., Thomas, D. S. G., Bullard, J. E. & Livingstone, I. Dune mobility and vegetation cover in the southwest Kalahari Desert. *Earth Surf. Proc. Landforms* **20,** 515–529 (1995).
8. Wasson, R. J. & Nanninga, P. M. Estimating wind transport of sand on vegetated surface. *Earth Surf. Proc. Landforms* **11,** 505–514 (1986).
9. Thomas, D. S. G. & Leason, H. Dunefield activity response to climate variability in the southwest Kalahari. *Geomorphology* **64,** 117–132 (2005).
10. International Panel on Climate Change (IPCC). *Climate Change 2001* (Cambridge Univ. Press, Cambridge, 2001).
11. Woodruff, W. P. & Armbrust, D. V. A monthly climatic factor for the wind erosion equation. *J. Soil Wat. Conserv.* **23,** 103–104 (1968).
12. Bauer, B. O., Yi, J., Namikas, S. L. & Sherman, D. J. Event detection and conditional averaging in unsteady aeolian systems. *J. Arid Environs* **39,** 345–375 (1998).
13. Wiggs, G. F. S., Thomas, D. S. G., Bullard, J. E. & Livingstone, I. Dune mobility and vegetation cover in the southwest Kalahari Desert. *Earth Surf. Proc. Landforms* **20,** 515–529 (1995).
14. Talbot, M. R. Late Pleistocene rainfall and dune building in the Sahel. *Palaeoecol. Afr.* **16,** 203–214 (1984).
15. Kar, A. Aeolian processes and bedforms in the Thar Desert. *J. Arid Environs* **25,** 83–96 (1993).
16. Bullard, J. E., Thomas, D. S. G., Livingstone, I. & Wiggs, G. F. S. Dunefield activity and interactions with climatic variability in the southwest Kalahari desert. *Earth Surf. Proc. Landforms* **22,** 165–174 (1997).
17. Muhs, D. R. & Maat, P. B. The potential response of eolian sands to greenhouse warming and precipitation reduction on the Great Plains of the USA. *J. Arid Environs* **25,** 905–918 (1993).
18. Lancaster, N. & Helm, K. A test of a climatic index of dune mobility using measurements from the southwestern United States. *Earth Surf. Proc. Landforms* **25,** 197–207 (2000).
19. Knight, M., Thomas, D. S. G. & Wiggs, G. F. S. Challenges of calculating dunefield mobility over the 21st century. *Geomorphology* **59,** 197–213 (2004).
20. Nakicenovic, N. & Swart, R. *IPCC Special Report on Emissions Scenarios* (IPCC, UNEP & WMO, Cambridge Univ. Press, Cambridge, 2000).
21. Summer, G., Homar, V. & Ramis, C. Precipitation seasonality in eastern and southern coastal Spain. *Int. J. Clim.* **21,** 211–247 (2001).
22. Korner, C. Biosphere responses to CO_2 enrichment. *Ecol. Appl.* **10,** 1590–1619 (2000).
23. Hulme, M. *Climate Change and Southern Africa* (CRU, Univ. of East Anglia, Norwich, 1996).
24. Thomas, D. S. G. & Shaw, P. A. Late Quaternary environmental change in central southern Africa: new data, synthesis, issues and prospects. *Quat. Sci. Rev.* **21,** 783–798 (2002).
25. Chepil, W. S. & Woodruff, N. P. The physics of wind erosion and its control. *Adv. Agron.* **15,** 211–302 (1963).
26. Tsoar, H. & Møller, J. T. in *Aeolian Geomorphology* (ed. Nickling, W. G.) 75–95 (Allen and Unwin, Boston, 1986).
27. Scanlon, T. M., Albertson, J. D., Caylor, K. K. & Williams, C. A. Determining land surface fractional cover from NDVI and rainfall time series for a savanna ecosystem. *Remote Sens. Environ.* **13,** 419–428 (2002).
28. Ringrose, S. & Mathieson, W. A Landsat analysis of range conditions in the Botswana Kalahari drought. *Int. J. Remote Sens.* **12,** 1023–1051 (1991).
29. Nicholson, S. E. & Kim, J. The relationship of the El Nino oscillation to African rainfall. *Int. J. Clim.* **17,** 117–135 (1997).

Supplementary Information is linked to the online version of the paper at www.nature.com/nature.

Acknowledgements We thank P. Coles for draughting figures, and the University of Sheffield for financial support to M.K. H. Viles supplied Namib weather data used in model validation.

Author Information Reprints and permissions information is available at npg.nature.com/reprintsandpermissions. The authors declare no competing financial interests. Correspondence and requests for materials should be addressed to D.S.G.T. (david.thomas@ouce.ox.ac.uk).